Synthesis and *Pseudomonas* Lipase Inhibition Study of Stereoisomers of Decahydro-2-naphthyl-N-*n*-butylcarbamate

Ming-Cheng Lin[1], Yu-Fang Shen[2] and Gialih Lin[2,*]

[1]*Department of Internal Medicine, Chung Shan Medical University Hospital, School of Medicine, Chung-Shan Medical University, Taichung 402, Taiwan,* [2]*Department of Chemistry, National Chung-Hsing University, Taichung 402, Taiwan*

Abstract: (2*S*,4a*R*,8a*S*)-*Cis*,*cis*-, (2*R*,4a*S*,8a*R*)-*cis*,*cis*-, *rac*-*cis*,*cis*-, and *rac*-*trans*,*cis*-decahydro-2-naphthyl-N-n-butylcarbamates are synthesized from condensation of (2*S*,4a*R*,8a*S*)-*cis*,*cis*-, (2*R*,4a*S*,8a*R*)-*cis*,*cis*-, *rac*-*cis*,*cis*-, and *rac*-*trans*,*cis*-decahydro-2-naphthols, respectively, with n-butyl isocyanate in the presence of triethylamine in dichloromethane. Optically pure (2*S*,4a*R*,8a*S*)-(-)- and (2*R*,4a*S*,8a*R*)-(+)-*cis*,*cis*-decahydro-2-naphthols are resolved by the porcine pancreatic lipase-catalyzed acetylation of decahydro-2-naphthols with vinyl acetate in *t*-butyl methyl ether. Absolute configurations of (2*S*,4a*R*,8a*S*)-(-)- and (2*R*,4a*S*,8a*R*)-(+)- *cis*,*cis*-decahydro-2-naphthols are determined from the ^{19}F NMR spectra of their Mosher's ester derivatives. (2*S*,4a*R*,8a*R*)-*Trans*,*cis*- and (2*R*,4a*S*,8a*S*)-*trans*,*cis*-decahydro-2-naphthols can't be resolved from the porcine pancreatic lipase-catalyzed acetylation of decahydro-2-naphthols with vinyl acetate in *t*-butyl methyl ether. For the inhibitory potency of *Pseudomonas* lipase, (2*S*,4a*R*,8a*S*)-*cis*,*cis*-decahydro-2-naphthyl-N-*n*-butylcarbamate is 3.5 times more potent than (2*R*,4a*S*,8a*R*)-*cis*,*cis*-decahydro-2-naphthyl-N-*n*-butylcarbamate; racemic *cis*,*cis*-decahydro-2-naphthyl-N-*n*-butylcarbamate is about the same with *trans*,*cis*-decahydro-2-naphthyl-N-*n*-butylcarbamate. These inhibitors also show similar effects on porcine pancreatic lipase.

Keywords: Lipase, stererospecificity, carbamates, inhibitors, resolutions.

INTRODUCTION

Lipases are lipolytic enzymes, which primarily hydrolyze ester bonds of triacylglycerols [1]. Lipases (EC 3.1.1.3) have been widely used in organic synthesis especially in resolution of many chiral secondary alcohols as the enantiomerically pure starting materials in asymmetric synthesis [2,3].

Many X-ray structures of lipases such as *Pseudomonas cepacia* lipase (PCL) and *Candida rugosa* lipase (CRL) have been reported [4-9]. Lipase usually contains a small α-helix or loop, referred to as the lid, which covers the active site pocket [4,6,7,10-14]. This conformation is termed the closed conformation. When the lipase is absorbed to an interface, the lid is displaced so that the active site becomes accessible to substrate [10]. This conformation is termed the open conformation. The structures of the free and bound lipase are believed to represent the start and end conformation in the interfacial activation process [15].

Recently, there has been increased interest in lipase inhibitors due to the use of Orlistat (Xenical®) [16]. Orlistat, whose original mechanism of action consists of the selective inhibition of gastrointestinal lipases, has been commercialized for the treatment of obesity. Orlistat is a chiral drug. Therefore, the stereoselctivity for lipase inhibition plays an important role in the design of novel drugs for management of obesity.

Aryl carbamates [17,18], 1,2-ethylene-di-*N*-alkylcarbamates [19], 1,2-cyclopentane-di-*N*-alkylcarbamates [20], and 1-acyloxy-3-*N*-*n*-octyl- carbamyl-benzenes [21] have been reported as potent inhibitors as *Pseudomonas species* lipase (PSL). We have synthesized (*R*)-(+)-*exo*-, (*S*)-(-)-*exo*-, (*R*)-(+)-*endo*-, and (*S*)-(-)-*endo*-2-norbornyl-N-*n*-butylcarbamates from optically pure (*R*)-(+)-*exo*-, (*S*)-(-)-*exo*-, (*R*)-(+)-*endo*-, and (*S*)-(-)-*endo*-2-norborneols which are kinetically resolved by porcine pancreatic lipase (PPL) in organic solvent [22,23]. (*R*)-(+)-*exo*-, (*S*)-(-)-*exo*-, (*R*)-(+)-*endo*-, and (*S*)-(-)-*endo*-2-Norbornyl N-*n*-butylcarbamates have shown high enantioselectivity for the inhibition of acetylcholinesterase and butyrylcholinesterase. In this paper, we further report that the stereoselectivity for lipase inhibitions by stereoisomers of decahydro-2-naphthyl-N-*n*-butylcarbamate.

Carbamate inhibitors have been characterized as the pseudo substrate inhibitors of CEase (Scheme **I**) [17-30]. In this paper, we also characterize all stereoisomers of decahydro-2-naphthyl-N-*n*-butylcarbamate as the pseudo substrate inhibitors of PSL and PPL.

Optically pure (2*S*,4a*R*,8a*S*)-(-)- and (2*R*,4a*S*,8a*R*)-(+)-*cis*,*cis*-decahydro-2- naphthols have been resolved from microbial hydrolysis of (±)-*cis*,*cis*-decahydro-2- naphthyl acetate by *Bacillus subtilis* [31]. For resolution of enantiomers of secondary alcohols, lipases (EC 3.1.1.3) have been widely chosen to use because lipases can be applied in organic solvent that is vey convenient to organic chemists [2, 3]. In this paper, we apply the lipase-catalyzed stereospecifically acetylation of one of enantiomers of (2*S*,4a*R*,8a*S*)-(-)- and (2*R*,4a*S*,8a*R*)-(+)-*cis*,*cis*-decahydro- 2-naphthols form a mixture of stereoisomers of decahydro-2-naphthols with vinyl acetate in *t*-butyl methyl ether.

*Address correspondence to this author at the Department of Chemistry, National Chung-Hsing University, Taichung 402, Taiwan;
Tel: +886-4-2284-0411; Ext 705; Fax: +886-4-2286-2547;
E-mail: gilin@dragon.nchu.edu.tw

0929-8665/11 $58.00+.00

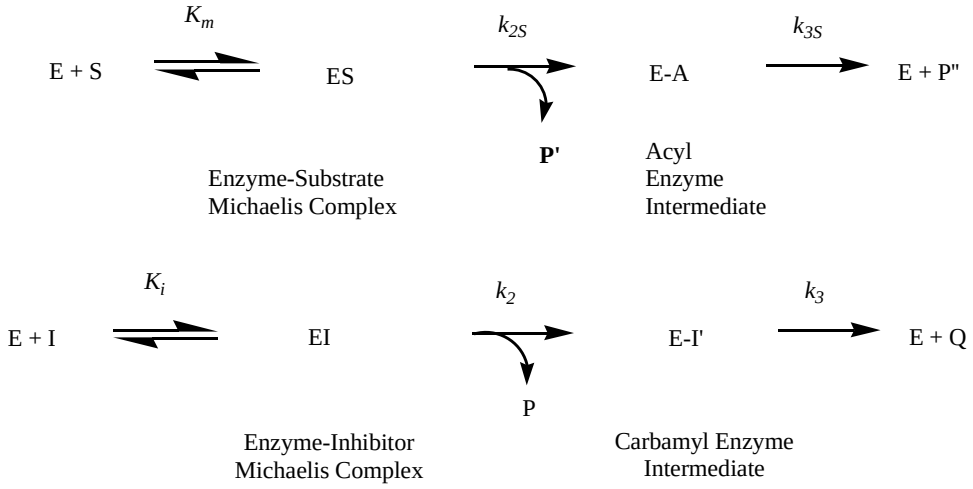

[a]E: enzyme; E-A: acyl enzyme; EI: enzyme-inhibitor Michaelis complex; E-I': carbamyl enzyme intermediate; ES: enzyme-substrate Michaelis complex; I: pseudo substrate inhibitor; k_2: carbamyl constant; k_3: decarbamylation constant; k_{2S}: formation rate constant of E-A; k_{3S}: deacylation constant of E-A; K_i: inhibition constant; K_m: Machaelis-Menten constant; P: product, decahydro-2-naphthol; P': product, p-nitrophenol; P'': product, butyrate; Q: product, butylcarbamic acid; S: substrate, PNPB.

Scheme I. Kinetic scheme for pseudo-substrate inhibitions of PSL by decahydro-2-naphthyl- N-n-butylcarbamates in the presence of substrate.[a]

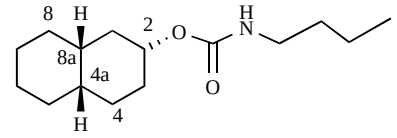

(2R,4aS,8aR)-cis,cis-decahydro-2-naphthyl-N-*n*-butylcarbamate

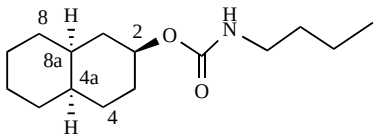

(2S,4aR,8aS)-cis,cis-decahydro-2-naphthyl-N-*n*-butylcarbamate

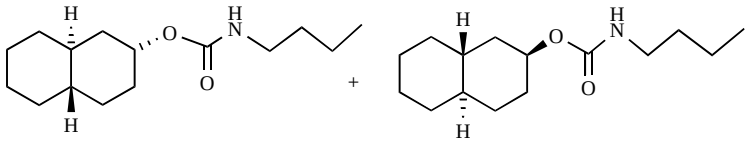

racemic-*trans,cis*-decahydro-2-naphthyl-N-*n*-butylcarbamate

Figure 1. Structures of (2S,4aR,8aS)-cis,cis-, (2R,4aS,8aR)-cis,cis-, and racemic trans,cis- decahydro-2-naphthyl- N-n-butylcarbamate.

MATERIALS AND METHODS

Materials

Pseudomonas species lipase (PSL), porcine pancreatic lipase (PPL), *p*-nitrophenyl butyrate (PNPB), and triton-X 100 (TX) were obtained from Sigma. Decahydro-2-naphthol, *n*-butyl isocyanate, triethylamine, $CDCl_3$, tetramethylsilane, *t*-butyl methyl ether, butanol, vinyl acetate, butyryl chloride, pyridine, and (*S*)-(+)-α-methoxy-α- trifluoromethyl- phenylacetyl chloride were purchased from Aldrich (USA). Silica gel and TLC plate were obtained from Merck (Germany). Hexane, CH_2Cl_2, ethyl acetate, and tetrahydrofuran were obtained from TEDIA (USA). Sodium dihydrogen phosphate (NaH_2PO_4:$2H_2O$), disodium hydrogen phosphate (Na_2HPO_4:$12H_2O$), hydrogen chloride (HCl), sodium hydroxide (NaOH), potassium hydroxide (KOH), calcium chloride ($CaCl_2$), and sodium chloride (NaCl) were purchased from UCW (Taiwan). Ethanol (95%) was obtained from Taiwan Tobacco & Liquid Corporation (Taiwan). All other chemicals were of the highest purity available commercially. All other chemicals were of the highest purity available commercially.

Instrumental Methods

^1H, ^{13}C, ^{19}F NMR spectra were recorded in $CDCl_3$ at 400, 100, and 377 MHz, respectively, with an internal reference tetramethylsilane (TMS) at 25 ^oC on a Varian Gemini 400 spectrometer. Mass spectra were recorded at 71 eV in a mass spectrometer (Joel JMS-SX/SX 102A). Elemental analyses were preformed on a Heraeus instrument. Optical rotation was recorded on a polarimeter (Perkin-Elmer 241).

SYNTHESIS

Kinetic resolution of (2*S*,4a*R*,8a*S*)-(-)- and (2*R*,4a*S*,8a*R*)-(+)-*cis,cis*- decahydro-2-naphthols (Fig. **2**).

To a *t*-butyl methyl ether (50 mL) solution of decahydro-2-naphthol (32.5 m mol) and vinyl acetate (10 mL), 30 g of porcine pancreatic lipase were added. The reaction mixture was shaken at 37 ^oC at 200 rpm for 72 h. This reaction

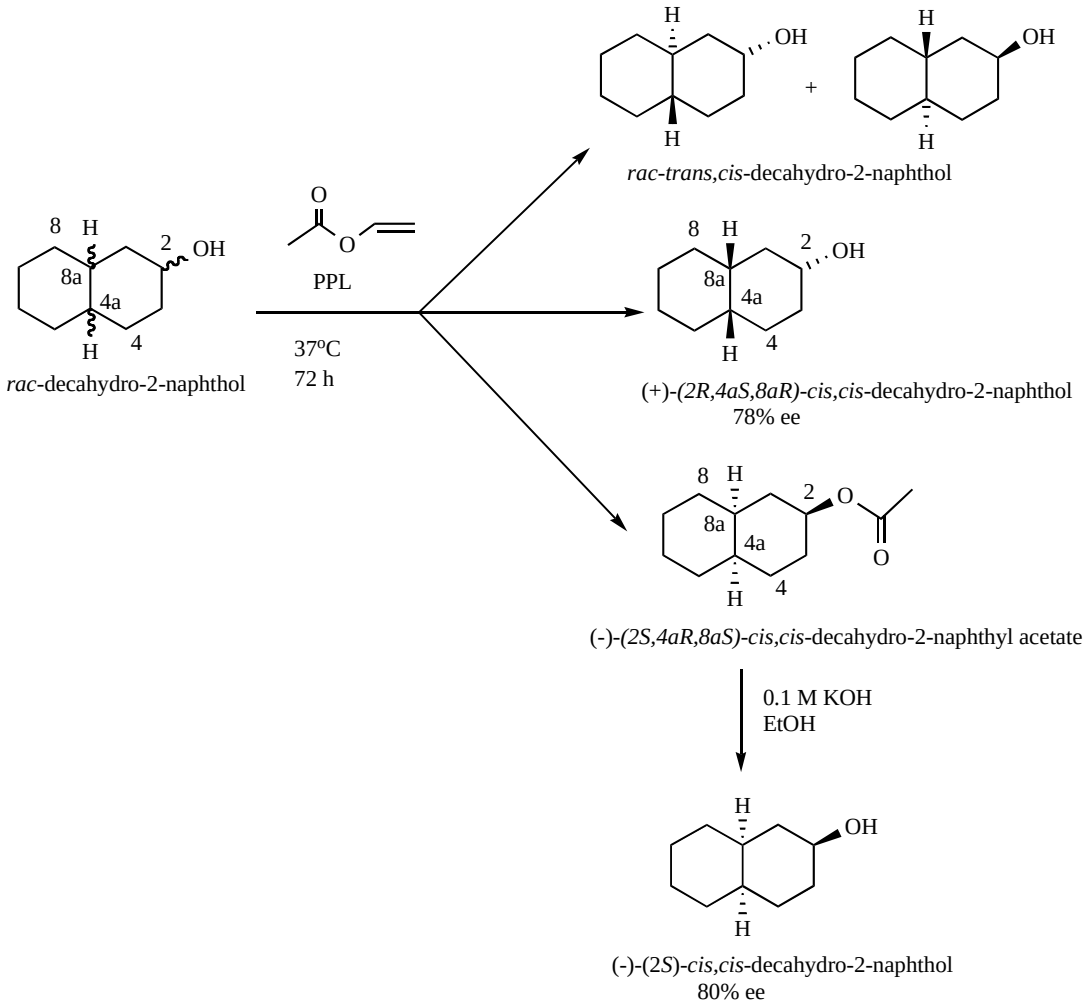

Figure 2. Kinetic resolution of (2S,4aR,8aS)-(-)- and (2R,4aS,8aR)-(+)-cis,cis- decahydro-2-naphthols from lipase catalyzed acetylation of racemic (±)- cis,cis-decahydro-2-naphthol with vinyl acetate.

yielded (2*S*,4a*R*,8a*S*)-(-)-*cis*,*cis*-decahydro-2-naphthyl acetate (33%) and recovered unreactive (2*R*,4a*S*,8a*R*)-(+)-*cis*,*cis*-decahydro-2-naphthol (35%) and racemic (±)-*trans*,*cis*-decahydro-2-naphthol (30%) (Fig. **2**). The optical purity of (2*R*,4a*S*,8a*R*)-(+)-*cis*,*cis*-decahydro-2-naphthol ($[\alpha]_D^{25}$ = +32.3 °) from this resolution was calculated to be 80% ($[\alpha]_D^{25}$ = +40.4 ° from literature [31]. (2*S*,4a*R*,8a*S*)- (-)-*cis*,*cis*-Decahydro-2-naphthol was obtained from the basic hydrolysis (0.1 M KOH) of (2*S*)-(-)-*cis*,*cis*-decahydro-2-naphthyl acetate in ethanol in 99% yield. The optical purity of (2*S*,4a*R*,8a*S*)-(-)-*cis*,*cis*-decahydro-2-naphthol ($[\alpha]_D^{25}$ = -32.7°) from this resolution was calculated to be 81% ($[\alpha]_D^{25}$ = -40.4 ° from literature [31].

The enantiomeric excess (e.e.) values of (2*R*,4a*S*,8a*R*)-(+)- and (2*S*,4a*R*,8a*S*)-(-)- *cis*,*cis*-decahydro-2-naphthols from the resolutions were calculated to be 78 and 80%, respectively, from the ^{19}F NMR spectra of their Mosher's esters (Fig. **3** and Table **1**).

In a NMR tube, condensation reaction of (2*R*,4a*S*,8a*R*)-(+)-*cis*,*cis*- decahydro-2-naphthol (5 mM) with the Mosher's chiral derivatizing agent (*S*)-(+)-α-methoxy-α-trifluoromethylphenylacetyl chloride [32] (5 mM) in $CDCl_3$ in the presence of pyridine (5 mM) at 25 °C for 24 h. The fluorine chemical shifts at -73.982 and -74.237 ppm with the integration ratio of 89/11 were assigned to be the fluorine atoms of (2*R*,4a*S*,8a*R*)- *and* (2*S*,4a*R*,8a*S*)- *cis*,*cis*-decahydro-2-naphthyl-(*S*)- α-methoxy-α-trifluoromethylphenyl acetates, respectively (Fig. **3**) [33, 34]. Therefore, the enantiomeric excess of (2*R*,4a*S*,8a*R*)-(+)-*cis*,*cis*-decahydro-2-naph-thol from the kinetic resolution by lipase catalysis (Fig. **2**) was calculated to be 78 % from integration of these two peaks (Fig. **3** and Table **1**).

(2*S*,4a*R*,8a*S*)-(-)-*cis*,*cis*-Decahydro-2-naphthol (5 mM) was condensed with the Mosher's chiral derivatizing agent (*S*)-(+)-α-methoxy-α-trifluoro-methylphenylacetyl chloride [32] (5 mM) in $CDCl_3$ in the presence of pyridine (5 mM) at 25 °C for 24 h. The fluorine chemical shifts at -74.024 and -74.279 ppm with the integration ratio of 10/90 were assigned to be the fluorine atoms of (2*R*,4a*S*,8a*R*)- and (2*S*,4a*R*,8a*S*)-*cis*,*cis*-decahydro-2-naphthyl-(*S*)-α-methoxy-α-trifluoromethylphenyl acetates, respectively. Therefore, the enantiomeric excess of (2*S*,4a*R*,8a*S*)-(-)-*cis*,*cis*- decahydro-2-naphthol from the kinetic resolution by lipase catalysis was calculated to be 80 % from integration of these two peaks (Fig. **3** and Table **1**).

Table 1. Enantiomeric Excess (%) and Optical Purity (%) for the Kinetic Resolution of Enantiomers of *Cis,cis*-decahydro-2-Naphthanol (Fig. 1) by Lipase in Organic Solvent

Compound	Enantiomeric Excess (%)[a]	Optical Purity (%)[b]
(2*R*,4a*S*,8a*R*)-(+)-*cis,cis*-decahydro-2-naphthol	78	80
(2*S*,4a*R*,8a*S*)-(-)-*cis,cis*-decahydro-2-naphthol	80	81

[a] Enantiomeric excess (%) was calculated from ratio of integration of fluorine chemical shifts of their Mosher's ester derivatives of ^{19}F NMR spectra.

[b]Optical purity (%) was calculated as 100 x $[\alpha]_{D}^{25}{}_{observed}$ / $[\alpha]_{D}^{25}{}_{literature}$.

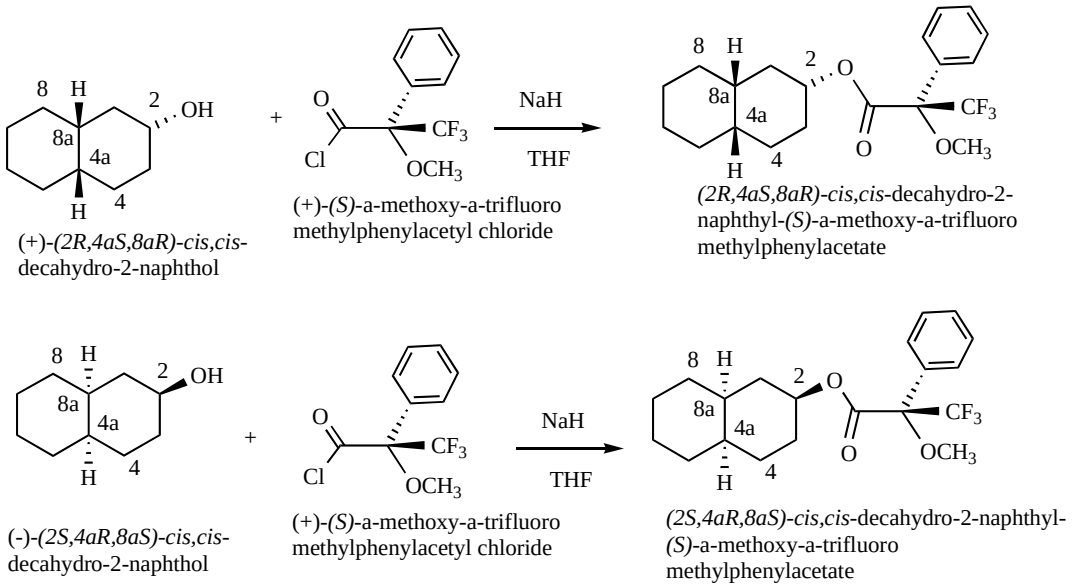

Figure 3. Determination of enantiomeric excess and absolute configuration of (2*S*,4a*R*,8a*S*)-(-)- *and* (2*R*,4a*S*,8a*R*)-(+)-*cis,cis*-decahydro-2-naphthols by ^{19}NMR spectra of their Mosher's ester derivatives. ^{19}F NMR spectra after the reaction of with *S*-(+)-α-methoxy-α-trifluoro-methylphenylacetyl chloride in the presence of pyridine in $CDCl_3$. The peaks at -73.982 and -74.237 ppm were assigned to be the fluorine chemical shifts of (2*R*,4a*S*,8a*R*)- and (2*S*,4a*R*,8a*S*)- *cis,cis*- (*S*)-α-methoxy-α-trifluoromethyl- phenylacetates, respectively.

(2*R*,4a*S*,8a*R*)-(+)- or (2*S*,4a*R*,8a*S*)-(-)-, or racemic (±)-*cis,cis*-decahydro-2-naphthol ^{1}H NMR ($CDCl_3$) δ0.80-1.80 (m, 16H, 1,3-8,4a,8a-decahydro-2-naphthyl *H*s), 3.03-3.09 (m, 1H, decahydro-2-naphthyl-C(2)*H*). ^{13}C NMR ($CDCl_3$) δ 22.5 (*C*-4), 26.2, 26.4 (*C*-6 and *C*-7), 30.6, 30.9 (*C*-5 and *C*-8), 32.0 (*C*-8a), 32.8 (*C*-3), 34.3, 34.7 (*C*-1 and *C*-4a), 74.0 (*C*-2). HRMS, exact mass: 154.1354; elemental analysis: calculated for $C_{10}H_{18}O$: C, 77.87; H, 11.76, found C, 77.78; H, 11.93.

(2*S*,4a*R*,8a*S*)-*cis,cis*-Decahydro-2-naphthylacetate ^{1}H NMR ($CDCl_3$) δ0.80-1.80 (m, 16H, 1,3-8,4a,8a-decahydro-2-naphthyl *H*s), 2.00 (s, 3H, acetyl methyl), 3.87-3.92 (m, 1H, decahydro-2-naphthyl-C(2)*H*). ^{13}C NMR ($CDCl_3$) δ 17.7 (acetyl methyl), 22.6 (*C*-4), 26.3, 26.4 (*C*-6 and *C*-7), 30.5, 30.8 (*C*-5 and *C*-8), 32.0 (*C*-8a), 32.7 (*C*-3), 34.2, 34.7 (*C*-1 and *C*-4a), 70.1 (*C*-2), 170.9 (acetyl *C*=O). HRMS, exact mass: 196.1460; elemental analysis: calculated for $C_{12}H_{20}O_2$: C, 73.43; H, 10.27, found C, 73.31; H, 10.34.

Synthesis of racemic *trans,cis*-, (2*R*,4a*S*,8a*R*)-*cis,cis*-, and (2*S*,4a*R*,8a*S*)- -*cis,cis*-decahydro-2-naphthyl-*N*-*n*-butycarbamates.

Racemic *trans,cis*-, (2*R*,4a*S*,8a*R*)-*cis,cis*-, (2*S*,4a*R*,8a*S*)-*cis,cis*-, and racemic *cis,cis*-decahydro-2-naphthyl-*N*-*n*-butycarbamates (Fig. **1**) were synthesized from condensation of the corresponding alcohol with *n*-butyl isocyanate in the presence of trethylamine in CH_2Cl_2 for 48h at 25 °C (70-80 yield).

Racemic *trans,cis*-decahydro-2-naphthyl-*N*-*n*-butycarbamate ^{1}H NMR (200 MHz, $CDCl_3$) δ 0.92 (t, J = 7.0 Hz, 3H, carbamate ω-C*H*$_3$), 1.20-2.00 (m, 20H, carbamate β- and γ-C*H*$_2$ and decahydro-2-naphthyl *H*s), 3.17 (dt, J = 6.2 and 6.8 Hz, 2H, carbamate α-C*H*$_2$), 3.85-3.90 (m, 1H, decahydro-2-naphthyl C(2)-*H*), 4.53 (br. s, 1H, carbamate NH). ^{13}C NMR (50.3 MHz, $CDCl_3$) δ 13.7 (carbamate ω-*C*H$_3$), 19.9 (carbamate β-*C*H$_2$), 26.5, 22.6, 28.2, 30.3, 32.1, 33.7 (decahydro-2-naphthyl *C*-3 to *C*-8), 33.7 (carbamate γ-*C*H$_2$), 37.2 (decahydro-2-naphthyl *C*-9), 37.6 (decahydro-2-naphthyl *C*-1), 40.6 (decahydro-2-naphthyl *C*-10), 42.7 (carbamate α-*C*H$_2$), 70.4 (decahydro-2-naphthyl *C*-2), 156.4 (carbamate *C*=O). HRMS, exact mass: 239.1889; elemental analysis: calculated for $C_{14}H_{25}NO_2$: C, 70.25; H, 10.53, found C, 70.19; H, 10.61.

(2*R*,4a*S*,8a*R*)-, (2*S*,4a*R*,8a*S*)-, or racemic *cis,cis*-decahydro-2-naphthyl- *N*-*n*-butycarbamate ^{1}H NMR (200 MHz, $CDCl_3$) δ 0.92 (t, J = 7 Hz, 3H, carbamate ω-C*H*$_3$), 1.20-2.00 (m, 20H, carbamate β- and γ-C*H*$_2$ and decahydro-2-naphthyl

Hs), 3.15 (dt, J = 6.2 and 6.8 Hz, 2H, carbamate α-C*H*$_2$), 4.53-4.59 (m, 1H, decahydro-2-naphthyl C(2)-*H*), 4.84 (br. s, 1H, carbamate NH). ^{13}C NMR (50.3 MHz, $CDCl_3$) δ 13.6 (carbamate ω-*C*H$_3$), 19.7 (carbamate β-*C*H$_2$), 26.4, 31.3, 33.0, 33.6, 34.4, 35.2 (decahydro-2-naphthyl *C*-3 to *C*-8), 32.0 (carbamate γ-*C*H$_2$), 38.5 (decahydro-2-naphthyl *C*-1), 40.6 (decahydro-2-naphthyl *C*-9), 40.9 (carbamate α-*C*H$_2$), 42.2 (decahydro-2-naphthyl *C*-10), 73.2 (decahydro-2-naphthyl *C*-2), 156.3 (carbamate *C*=O). HRMS, exact mass: 239.1890; elemental analysis: calculated for $C_{14}H_{25}NO_2$: C, 70.25; H, 10.53, found C, 70.20; H, 10.59.

Data Reduction

Origin (version 6.0) was used for linear and nonlinear least-squares curve fittings.

Lipase Inhibition

Lipase inhibition reactions were determined as described by Hosie et asl. [17-30]. PSL-or PPL-catalyzed hydrolysis of PNPB in the presence of a carbamate inhibitor was followed continuously at 410 nm on the UV-visible spectrometer. The temperature was maintained at 25.0 ^{o}C by a refrigerated circulating water bath. All reactions were preformed in sodium phosphate buffer (1 mL, 0.1 M, pH 7.0) containing NaCl (0.1 M), CH_3CN (2% by volume), detergent triton-X 100 (TX) (0.5% by weight), substrate PNPB (0.1 mM), and varying concentration of the inhibitors. Requisite volumes of stock solution of substrate PNPB and the inhibitor in acetonitrile were injected into reaction buffer via a pipet. PSL or PPL was dissolved in sodium phosphate buffer (0.1 M, pH 7.0). Carbamate inhibitors racemic *trans*,*cis*-, (2*R*,4a*S*,8a*R*)-*cis*,*cis*-, (2*S*,4a*R*,8a*S*)- -*cis*,*cis*-, and racemic *cis*,*cis*-decahydro-2-naphthyl-*N*-*n*-butycarbamates were characterized as the pseudo or alternate substrate inhibitors of PSL and PPL (Scheme I and Equation 1) [17-30]. The carbamylation stage was rapid compared to subsequent decarbamylation ($k_2 >> k_3$), thus the two steps are easily resolved kinetically. The apparent inhibition constant (1+[S]/K_m) K_i and carbamylation constant (k_2) were obtained from the nonlinear least-squares curve fitting of the k_{app} vs. [I] plot against Eq. (1) (Fig. **5**). The inhibition constant K_i was then calculated form the apparent inhibition constant when both [S] and K_m values for the PSL-catalyzed hydrolysis of PNPB were known (Table 2). The K_m value for the PSL catalyzed hydrolysis of PNPB was 100±20 μM obtained from Michaelis-Menten equation. The bimolecular rate constant, $k_i = k_2/K_i$, was related to overall inhibitory potency.

$$k_{app} = k_2 [I] / (K_i (1 + [S] / K_m)o + [I]) \quad (1)$$

Duplicate sets of data were collected for each inhibitor concentration.

Molecular Modeling

Molecular structures shown in Figs. **4** and **6** were depicted from the molecular structures after MM-2 energy minimization (minimum root mean square gradient was set to be 0.01) by CS Chem 3D (version 6.0).

Cytotoxicity Test *In Vitro*

For this experiment in 96-well white plate, 10000 MDCK cells were seeded per well and incubated for 24 hours at 37 ^{o}C. After 24 hours, MDCK cells were incubated with medium containing 0.04 % (weight) inhibitors or drugs. The number of metabolically viable cells was determined by the Celltiter-Glo^{TM} luminescent cell viability assay (Promega) after 48 hours. MDCK cells were grown in Dulbecco's Modified Eagle Medium (DMEM) containing 10% fetal bovine serum (FBS). Cells were maintained at 37 °C and 5% CO_2.

RESULTS AND DISCUSSION

Optically pure (2*S*,4a*R*,8a*S*)-(-)- and (2*R*,4a*S*,8a*R*)-(+)-*cis*,*cis*- decahydro-2-naphthols are resolved from the porcine pancreatic lipase (PPL)-catalyzed acetylation of decahydro-2-naphthols with vinyl acetate in *t*-butyl methyl ether (Fig. **2**). The enantiomeric excess (e.e.) values of (2*S*,4a*R*,8a*S*)-(-)- and (2*R*,4a*S*,8a*R*)-(+)-*cis*,*cis*-decahydro-2-naphthols from this resolution are calculated to be 78 and 80%, respectively, from the ^{19}F NMR spectra of their Mosher's ester derivatives (Fig. **3** and Table **1**) [32-34]. Superimposition of (2*S*,4a*R*,8a*S*)-(-)- and (2*R*,4a*S*,8a*R*)-(+)-*cis*,*cis*-decahydro-2-naphthols into the active site of acetyl enzyme suggests that the decahydro-2-naphthyl ring of (2*S*,4a*R*,8a*S*)-(-)- *cis*,*cis*-decahydro- 2-naphthol is fit well into the leaving group binding site of the enzyme and the hydroxyl group of (2*S*,4a*R*,8a*S*)-(-)- *cis*,*cis*-decahydro-2-naphthol is at the right position to attack the carbonyl carbon of acetyl enzyme (Fig. **4**). On the other hand, the decahydro-2-naphthyl ring of (2*R*,4a*S*,8a*R*)-(+)-*cis*,*cis*-decahydro- 2-naphthol is not fit well into the leaving group binding site of the enzyme, extending to the entrance (mouth) of the active site. Thus, the hydroxyl group of (2*R*,4a*S*,8a*R*)-(+)-*cis*,*cis*- decahydro-2-naphthol is away from the right position to attack the acetyl enzyme.

Optically pure (2*S*,4a*R*,8a*R*)- and (2*R*,4a*S*,8a*S*)-(+)-*trans*,*cis*- decahydro-2-naphthols can not be resolved from the porcine pancreatic lipase-catalyzed acetylation of decahydro-2-naphthols with vinyl acetate in *t*-butyl methyl ether. Therefore, the PSL inhibition by *trans*,*cis*-decahydro-2-naphthyl-N-*n*- butylcarbamate (Fig. **1**) is studied in its racemate form.

(2*S*,4a*R*,8a*S*)-*Cis*,*cis*-, (2*R*,4a*S*,8a*R*)-*cis*,*cis*-, racemic *cis*,*cis*-, and racemic *trans*,*cis*-decahydro-2-naphthyl-N-*n*-butylcarbamates (Fig. **1**) are all characterized as pseudo substrate inhibitors of PSL (Scheme **I**, Equation **1**, Fig. **5**, and Table **2**) [17-30]. Among all carbamate inhibitors in this study, (2*R*,4a*S*,8a*R*)-*cis*,*cis*- decahydro-2-naphthyl-N-*n*-butyl-carbamate is the most potent inhibitor of PSL (Table 2). Superimposition of (2*R*,4a*S*,8a*R*)-*cis*,*cis*-, (2*S*,4a*R*,8a*R*)-*cis*,*cis*-, (2*S*,4a*R*,8a*R*)- *trans*,*cis*-, and (2*R*,4a*S*,8a*S*)-*trans*,*cis*-decahydro-2-naphthyl-N-*n*-butylcarbamates and triacylglycerol into the active site of PSL is modeled (Fig. **6**). The *sn*-1 or *sn*-3 acyl chain of triacylglycerol and the carbamate moieties of the inhibitors are fit into the acyl chain binding site (ACS) of the enzyme [5]. The *sn*-1 or *sn*-3 acyl carbonyl oxygen atom of the triacylglycerol and the carbamate

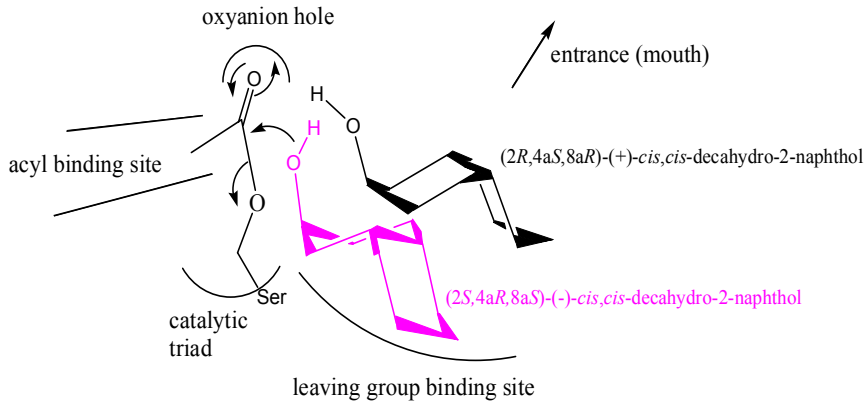

Figure 4. Superimposition of (2*S*,4a*R*,8a*S*)-(-)- and (2*R*,4a*S*,8a*R*)-(+)- *cis*,*cis*-decahydro-2-naphthols into the active site of acetyl PPL. The decahydro-2-naphthyl ring of (2*S*,4a*R*,8a*S*)-(-)-*cis*,*cis*-decahydro-2-naphthol fits well into the leaving group binding site of lipase and the hydroxyl group of (2*S*,4a*R*,8a*S*)-(-)- *cis*,*cis*-decahydro-2-naphthol is at the right position to attack the acetyl enzyme. On the other hand, (2*R*,4a*S*,8a*R*)-(+)-*cis*,*cis*- decahydro-2-naphthol does not fit well into the leaving group binding site of lipase, extending to the entrance (mouth) of the active site. Thus, the hydroxyl group of (2*R*,4a*S*,8a*R*)-(+)-*cis*,*cis*- decahydro-2-naphthol is away from the position to attack the acetyl enzyme.

Table 2. The k_2, K_i and k_i Vlaues[a] of the PSL Inhibitions by Stereoisomers of Decahydro-2-naphthyl-N-*n*-butylcarbamates

Inhibitors[b]	K_i (μM)	k_2 ($10^{-3} s^{-1}$)	k_i ($10^3 M^{-1}s^{-1}$)	*Enantioselectivity*
(2*R*,4a*S*,8a*R*)-*cis*,*cis*-	1.3±0.2	0.43±0.02	3.3±0.5	3.5
(2*S*,4a*R*,8a*S*)-*cis*,*cis*-	4.2±0.3	0.40±0.02	0.95±0.07	1.0
rac-(±)-*cis*,*cis*-	2.5±0.2	0.42±0.02	1.7±0.1	1.8
rac-(±)-*trans*,*cis*	4.0±0.4	0.60±0.03	1.5±0.2	-

[a] Obtained from the nonlinear least-squares curve fittings of k_{app} vs. [I] plot against Eq. (1).
[b] (2*R*,4a*S*,8a*R*)- *cis*,*cis*-, (2*S*,4a*R*,8a*S*)-*cis*,*cis*-, and rac-(±)-*cis*,*cis*- stand for (2*R*,4a*S*,8a*R*)-, (2*S*,4a*R*,8a*S*)-, and racemic *cis*,*cis*-decahydro-2-naphthyl-N-*n*- butylcarbamates. Rac-(±)-*trans*,*cis* stand for (2*R*,4a*S*,8a*S*)- and (2*S*,4a*R*,8a*R*)-*trans*,*cis*-decahydro-2-naphthyl-N-*n*- butylcarbamates.

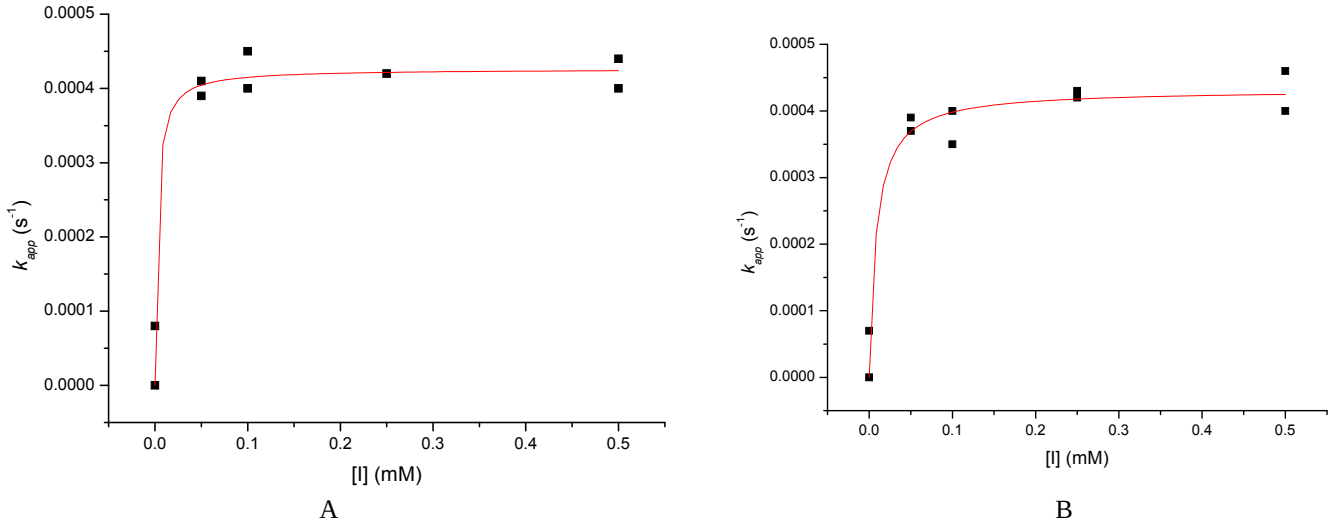

Figure 5. Nonlinear least-squares curve fittings of k_{app} vs. inhibitor concentration ([I]) plot against Eq. (1) for the pseudo-substrate inhibition of PSL by (**A**) (2*R*,4a*S*,8a*R*)- *cis*,*cis*-decahydro-2-naphthyl-N-n-butylcaarbamate and (**B**) (2*S*,4a*R*,8a*S*)- *cis*,*cis*-decahydro-2-naphthyl-N-n-butylcaarbamate. The parameters of the fit were (**A**) k_2 = 0.00043 ± 0.00002 s^{-1} , K_i = 1.3 ±0.2 μM, and R= 0.98064 and (**B**) k_2 = 0.00040± 0.0003 s^{-1} , K_i =4.2 ± 0.3 μM, and R= 0.97847.

carbonyl oxygen atom are fit into the oxyanion hole of the enzyme [5-7]. The *sn*-1 or *sn*-3 acyl carbonyl carbon atom of the triacylglycerol and the carbamate carbonyl carbon atom are fit into the correct position for Ser87 of the catalytic triad of the enzyme to attack [5-7].

For stereospecificity of the PSL inhibition, (2*R*,4a*S*,8a*R*)-*cis*,*cis*-decahydro-2- naphthyl-N-*n*-butylcarbamate is 3.5 times more potent than (2*S*,4a*R*,8a*S*)-*cis*,*cis*- decahydro-2-naphthyl-N-*n*-butylcarbamate (Table 2). Superimposition of both enantiomers of *cis*,*cis*-decahydro-2-naphthyl-N-*n*-

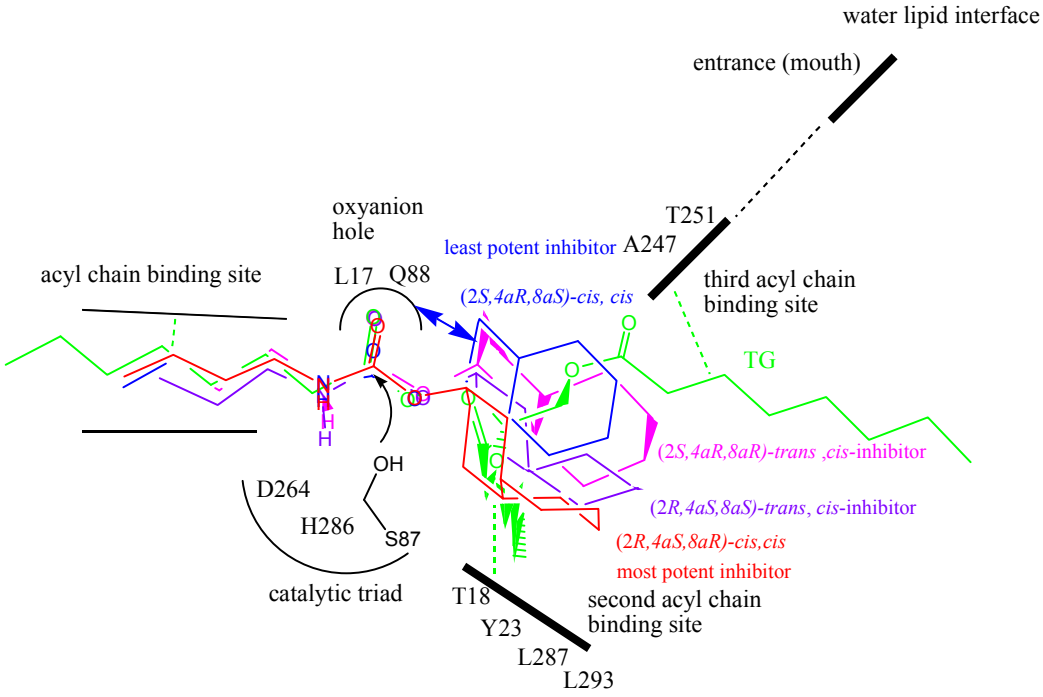

Figure 6. Superimposition of (2*S*,4a*R*,8a*S*)-*cis*,*cis*-, (2*R*,4a*S*,8a*R*)-*cis*,*cis*- , (2*S*,4a*R*,8a*R*)-*trans*,*cis*-, (2*R*,4a*S*,8a*S*)-*trans*,*cis*-decahydro-2-naphthyl- N-*n*-butylcarbamates and triacylglycerol into the active site of PSL [5]. The decahydro-2-naphthyl ring of (2*S*,4a*R*,8a*S*)-*cis*,*cis*-isomer unfavorably interacts with the oxyanion hole of the enzyme, but that of (2*R*,4a*S*,8a*R*)-*cis*,*cis*-isomer does not. Furthermore, the decahydro-2-naphthyl ring of (2*R*,4a*S*,8a*R*)-cis,cis-isomer may bind well into the second acyl chain of the enzyme.

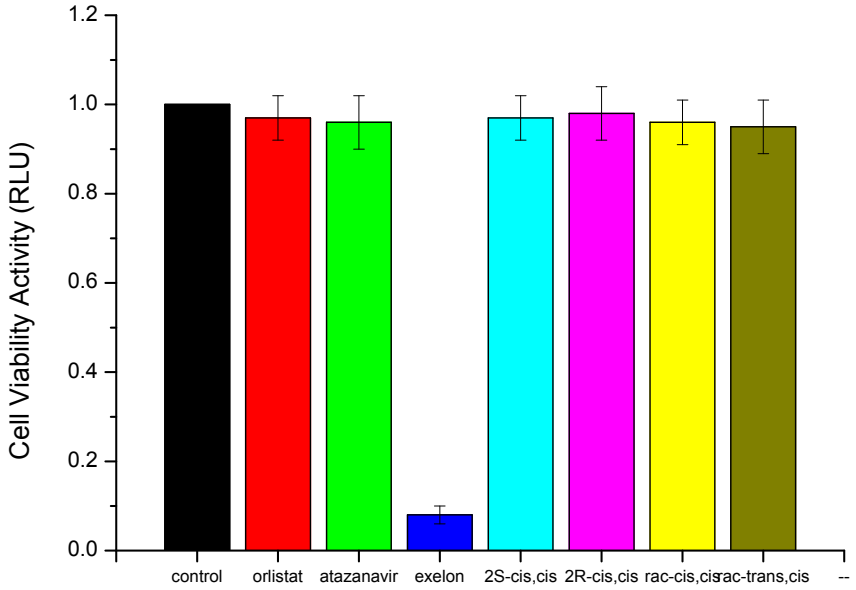

Figure 7. MCDK cell viability activity [relative light unit (RLU)] for Olistat, Atazanavir, Exelon, and (2*S*,4a*R*,8a*S*)-*cis*,*cis*-, (2*R*,4a*S*,8a*R*)-*cis*,*cis*-, racemic-*cis*,*cis*-, and racemic-*trans*,*cis*-decahydro-2-naphthyl- N-*n*-butylcarbamates determined by the Celltiter-Glo™ luminescent cell viability assay (Promega).

butylcarbamate into the active site of PSL indicates that the decahydro-2-naphthyl rings of (2*S*,4a*R*,8a*S*)-*cis*,*cis*-isomer is strongly repulsive with the oxyanion hole of PSL [5] suggesting that this unfavorable interaction makes (2*S*,4a*R*,8a*S*)-*cis*,*cis*-isomer become the least potent inhibitor (Fig. **6**). On the other hand, the decahydro-2-naphthyl rings of (2*R*,4a*S*,8a*R*)-*cis*,*cis*-isomer does not have this unfavorable repulsions and may interact well with the second acyl chain binding site (SACS) of the enzyme [5].

The inhibitory potency of *rac*-*trans*,*cis*-isomer is between those of (2*S*,4a*R*,8a*S*)-*cis*,*cis*- and (2*R*,4a*S*,8a*R*)-*cis*,*cis*-isomers (Table 2). Superimposition of (2*S*,4a*R*,8a*R*)-*trans*,*cis*- and (2*R*,4a*S*,8a*S*)-*trans*,*cis*-isomers into the active site of

PSL suggests that the decahydro-2-naphthyl rings of both *trans*,*cis*-inhibitors are binding to where are between those of enantiomers of *cis*,*cis*-isomers (Fig. **6**).

These inhibitors also show similar effects on porcine pancreatic lipase and bovine bile salt activated lipase (or cholesterol esterase) since all enzymes mentioned above are belong to serine hydrolase and have similar structures.

For the cytoxicity test *in vitro*, all stereoisomers of decahydro-2-naphthyl-N-*n*- butylcarbamate, Orlistat, and Atazanvir (anti-virus drug) show little cytotoxicity on Madin-Darby Canine Kidney (MDCK) cells (Fig. **7**). Although anti-Alzheimer's disease drug Exelon is also a carbamate compound, Exelon shows high cytotoxicity on MDCK cells *in vitro*.

In summary, optically pure (2*S*,4a*R*,8a*S*)-(-)- and (2*R*, 4a*S*,8a*R*)-(+)-*cis*,*cis*- decahydro-2-naphthols are resolved from the lipase-catalyzed acetylation reaction. For PSL inhibition, (2*S*,4a*R*,8a*S*)-*cis*,*cis*-decahydro-2-naphthyl-N-*n*-butylcarbamate is 3.5 times less potent than (2*R*,4a*S*,8a*R*)-*cis*,*cis*-decahydro-2-naphthyl-N-*n*- butylcarbamate due to the unfavorable repulsion between the former inhibitor and the enzyme.

REFERENCES

[1] Svendsen, A. In: Lipases. Their structure biochemistry and application; Woolley, P.; Petersen, S. B., Ed.; Cambridge University Press: Cambridge; 1994; pp.1-21.

[2] Boland, W.; Frößl, C.; Lorenz, N. Esterolytic and lipolytic enzymes in organic synthesis. *Synthesis*, **1991,** *12*, 1049-1072.

[3] Theil, F. Lipase-supported synthesis of biologically active compounds. *Chem. Rev.*, **1995,** *95*, 2203-2227.

[4] van Tilbeurgh, H.; Egloff, M.-P.; Martinez, C.; Rugani, N.; Verger, R.; Cambillau, C. Interfacial activation of the lipase-procolipase complex by mixed micelles revealed by X-ray crystallography. *Nature*, **1993,** *362*, 814-820.

[5] Lang, D. A.; Mannesse, M. L. M.; DeHaas, G. H.; Verheij, H. M.; Dijkstra, B. W. Structural basis of the chiral selectivity of *Pseudomonas cepacia* lipase. *Eur. J. Biochem.*, **1998,** *254*, 333-340.

[6] Schrag, J. D.; Li, Y.; Cygler, M.; Lang, D.; Burgdorf, T.; Hecht, H.-J.; Schmid, R.; Schomburg, D.; Rydel, T. J.; Oliver, J. D.; Strickland, L. C.; Dunaway, C. M.; Larson, S. B.; Day, J.; McPherson, A. The open conformation of *Pseudomonas* lipase. *Structure*, **1997,** *5*,187-202.

[7] Kim, K. K.; Song, H. K.; Shin, D. H.; Hwang, K. Y.; Suh, S. W. The crystal structure of a triacylglycerol lipase from *Pseudomonas cepacia* reveals a highly open conformation in the absence of a bound inhibitor. *Structure*, **1997,** *5*, 173-185.

[8] Grochulski, P.; Bouthillier, F.; Kazlauskas, R. J.; Serreqi, A. N.; Schrag, J. D.; Ziomek, E.; Cygler, M. Analogs of reaction intermediates identify a unique substrate binding site in *Candida rugosa* lipase. *Biochemistry*, **1994,** *33*, 3494-3500.

[9] Luic, M.; Tomic, S.; Lescic, I.; Liubovic, E.; Sepac, D.; Sunjic, V.; Vitale, L.; Saenger, W.; Kojic-Prodic, B. Complex of *Burkholderia cepacia* lipase with transition state analogue of 1-phenoxy-2-acetoxybutane. Biocatalytic, structural and modeling study. *Eur. J. Biochem*., **2001,** *268*, 3964-3973.

[10] Brozozowski, A. M.; Derewenda, U.; Derewenda, Z. S.; Dodson, G. G.; Lawson, D. M.; Turkenburg, J. P.; Bjorkling, F.; Huge-Jensen, B.; Patkar, S. A.; Thim, L. A model for interfacial activation in lipase from structure of a fungal lipase-inhibitor complex. *Nature*, **1991,** *351*, 491-494.

[11] Brady, L.; Brzozowski, A. M.; Derewenda, Z. S.; Dodson, E.; Dodson, G. ; Tolley, S.; Turkenburg, J. P.; Christiansen, L.; Huge-Jensen, B.; Norskov, L.; Thim, L.; Menge, U. A serine protease triad forms the catalytic center of a triacylglycerol lipase. *Nature*, **1990,** *343*, 767-770.

[12] Pleiss, J.; Fischer, M.; Schmid, R. D. Anatomy of lipase binding sites: the scissile fatty acid binding site. *Chem. Phys. Lipids*, **1998,** *93*, 67-80.

[13] Cavalier, J.-F.; Buono, G.; Verger, R. Covalent inhibition of digestive lipases by chiral phosphates. *Acc. Chem. Res.*, **2000,** *33*, 579-589.

[14] Svendsen, A. Lipase protein engineering. *Biochim. Biophys. Acta*, **2000,** *1543*, 223-238.

[15] Derewenda, Z. S. A twist in the tale of lipolytic enzymes. *Nat. Struct. Biol.* **1995**, *2*, 347-349.

[16] Parker, K. L.; Schimmer, B. P. In: Goodman and Gilman's The Pharmacological Basis of Therapeutics; 11th edition; Brunton, L. L.; Lazo, J. S.; Parker, K. L. Eds.; McGraw-Hill: New York, 2005.

[17] Lin, G.; Chen, G.-H.; Lin, Y.-F.; Su, L.-H.; Liao, P.-S. Highly potent and selective 4,4'-biphenyl-4-acylate-4'-*N*-*n*-butylcarbamate inhibitors as *Pseudomonas species* lipase. *Eur. J. Lipid Sci. Tech*., **2005,** *107*, 65-73.

[18] Lin, G.; Liao, W.-C.; Ku, Z.-H. Quantitative structure-activity relationships for the pre-steady state of *Pseudomonas species* lipase inhibitions by *p*-nitrophenyl-*N*- substituted carbamates. *Protein J*., **2005,** *24*, 201-207.

[19] Lin, M.-C.; Lu, C.-P.; Cheng, Y.-R.; Lin, Y.-F.; Lin, C.-S.; Lin, G. Inhibition or activation of Pseudomonas species lipase by 1,2-ethylene-di-*N*-alkylcarbamates in detergents. *Chem. Phys. Lipids*, **2007,** *146*, 85-93.

[20] Lin, G.; Lai, F.-H.; Tsai, B.-I ; Hsieh, C.-W.; Tsai, H.-J. Probing conformations of the glycerol backbones of triacyglycerols in the active site of lipase by 1,2-cyclopentane- carbamates: the *meso* effect for the enzyme inhibition. *J. Mol. Catal. B Enzym.*, **2006,** *40*, 86-92.

[21] Chiou, S.-Y.; Yu, G.-Y.; Lin, G. QSAR for Inhibition of *Pseudomonas Species* Lipase by 1-Acyloxy-3-*N*-*n*-octylcarbamylbenzenes. *QSAR Comb. Sci.*, **2009,** *28*, 267-273.

[22] Chiou, S.-Y.; Huang, C.-F.; Yeh, S.-J.; Chen, I-R.; Lin, G. Synthesis of enantiomers of exo-2-norbornyl-N-n-butylcarbamate and endo-2-norbornyl-N-*n*-butylcarbamate for stereoselective inhibition of acetylcholinesterase. *Chirality*, **2010,** *22*, 267-274.

[23] Chiou, S.-Y.; Huang, C.-F.; Yeh, S.-J.; Chen, I-R.; Lin, G. Stereoselective inhibition of butyrylcholinesterase by enantiomers of exo- and endo-norbornyl-N-n-butylcarbamates. *J. Enzym. Inhib. Med. Chem.*, **2010,** *25*, 13-20.

[24] Hosie, L.; Sutton, L. D.; Quinn, D. M. *p*-Nitrophenyl and cholesteryl-N-alkyl carbamates as inhibitors of cholesterol esterase. *J. Biol. Chem.*, **1987,** *262*, 260-264.

[25] Feaster, S. R.; Lee, K.; Baker, N.; Hui, D. Y.; Quinn, D. M. Molecular recognition by cholesterol esterase of active site ligands: structure-reactivity effects for inhibition by aryl carbamates and subsequent carbamylenzyme turnover. *Biochemistry*, **1996**, *35*, 16723-16734.

[26] Feaster, S. R.; Quinn, D. M. Mechanism-based inhibitors of mammalian cholesterol esterase. *Methods Enzymol.*, **1997,** *286*, 231-252.

[27] Pietsch, M.; Gütschow, M. Alternate substrate inhibition of cholesterol esterase by thieno[2,3-d][1,3]oxazin-4-ones. *J. Biol. Chem.*, **2002,** *277*, 24006-24013.

[28] Pietsch, M.; Gütschow, M. Syntehsis of tricyclic 1,3-oxazin-4-ones and kinetic analysis of cholesterol esterase and acetylcholinesterase inhibition. *J. Med. Chem.*, **2005,** *48*, 8270-8288.

[29] Lin, G.; Lai, C.-Y. Hammett analysis of the inhibition of pancreatic cholesterol esterase by substituted phenyl-*N*-butylcarbamate. *Tetrahedron Lett.*, **1995,** *36*, 6117-6120.

[30] Lin, G.; Lai, C.-Y. Linear free energy relationships of the inhibition of pancreatic cholesterol esterase by 4-nitrophenyl-*N*-alkylcarbamate *Tetrahedron Lett.*, **1996,** *37*, 193-196.

[31] Oritani, T.; Yamashita, K.; Kabuto, C. Enantioselectivity of microbial hydrolysis of (±)-decahydro-2-naphthyl acetates. *J. Org. Chem.* **1984,** *49*, 3689-3694.

[32] Dale, J. A.; Mosher, H. S. Nuclear magnetic resonance enantiomer reagents. Configurational correlations *via* nuclear magnetic resonance chemical shifts of diastereomeric mandelate, *O*-methylmandelate, and α-methoxy-α- trifluoromethylphenylacetate (MTPA) esters. *J. Am. Chem. Soc.*, **1973,** *95*, 512-519.

[33] Takahashi, T.; Fukuishima, A.; Tanaka, Y.; Takeuchi, Y.; Kabuto, K.; Kabuto, C. CFTA, a new efficient agent for determination of absolute configurations of chiral secondary alcohols. *Chem. Commun.*, **2000,** 788-789.

[34] Takahashi, T.; Kameda, H.; Kamei, T.; Ishizaki, M. Synthesis of 1-fluoroindan-1-carboxylic acid (FICA) and its properties as a chiral derivatizing agent. *J. Fluorine Chem.*, **2006,** *127*, 760-768.

Received: March 22, 2011 **Revised: May 2, 2011** **Accepted: May 2, 2011**